Spectroscopy of 3, 4, 9, 10-perylenetetracarboxylic dianhydride (PTCDA) attached to rare gas samples: Clusters vs. bulk matrices. II. Fluorescence emission spectroscopy

Matthieu Dvorak, Markus Müller, Tobias Knoblauch, Oliver Bünermann, Alexandre Rydlo et al.

Additional information on J. Chem. Phys.

Journal Homepage: http://jcp.aip.org/

Journal Information: http://jcp.aip.org/about/about_the_journal

Top downloads: http://jcp.aip.org/features/most_downloaded

Information for Authors: http://jcp.aip.org/authors

Spectroscopy of 3, 4, 9, 10-perylenetetracarboxylic dianhydride (PTCDA) attached to rare gas samples: Clusters vs. bulk matrices. II. Fluorescence emission spectroscopy

Matthieu Dvorak,[1] Markus Müller,[1] Tobias Knoblauch,[2] Oliver Bünermann,[1,3] Alexandre Rydlo,[4] Stefan Minniberger,[4] Wolfgang Harbich,[4] and Frank Stienkemeier[1]

[1]*Physikalisches Institut, Universität Freiburg, Hermann-Herder-Str. 3, D-79104 Freiburg, Germany*
[2]*1. Physikalisches Institut, Universität Stuttgart, Pfaffenwaldring 57, 70550 Stuttgart, Germany*
[3]*Institut für Physikalische Chemie, Georg-August-Universität, Tammannstr. 6, 37077 Göttingen, Germany*
[4]*Institut de Physique des Nanostructures, École Polytechnique Fédérale de Lausanne (EPFL), CH-1015 Lausanne, Switzerland*

The interaction between 3, 4, 9, 10-perylenetetracarboxylic dianhydride (PTCDA) molecules and solid rare gas samples is studied by means of fluorescence emission spectroscopy. Laser-excited PTCDA-doped large argon, neon, and para-hydrogen clusters along with PTCDA embedded in helium nanodroplets are spectroscopically characterized with respect to line broadening and shifting. A fast non-radiative relaxation is observed before a radiative decay in the electronic ground state takes place. In comparison, fluorescence emission studies of PTCDA embedded in bulk neon and argon matrices result in much more complex spectral signatures characterized by a splitting of the different emission lines. These can be assigned to the appearance of site isomers of the surrounding matrix lattice structure. © *2012 American Institute of Physics*. [http://dx.doi.org/10.1063/1.4759445]

I. INTRODUCTION

In order to achieve highly resolved and clean electronic spectra, it is desirable to prepare isolated molecules at low temperatures. For many decades, the isolation in cryogenic matrices has been developed as an experimental technique to perform spectroscopy on vibrationally and rotationally cold species.[1] However, the drawback of matrix isolation is the interaction of the molecule with the environment, leading to broadenings and shifts of the spectral features.[2] Furthermore, broadening effects induced by the environmental temperature complicate even more the measurements and their interpretation. One way to limit both of these effects is to use rare gas matrices. The interaction between a chromophore and, e.g., an argon or neon matrix is much weaker than for other solid substrates and their achievable low temperatures contribute to a drastic improvement in spectroscopic resolution. For this reason, many studies on rare gas matrices doped with atoms and smaller molecules have already been published (a compendium of these molecules and their spectral features can be found in Ref. 3). Some larger polycyclic aromatic hydrocarbon (PAH) molecules and their ions, embedded in argon or in neon matrices have already been studied: C_{60},[4] naphthalene,[5] phenanthrene,[6] pentacene,[7] 9,10-dichloroanthracene,[8] benzo[g,h,i]perylene,[9] and perylene.[10,11] However, in spite of the improvements resulting from the use of rare gas matrices, the effect of the matrix environment which stabilizes the guest molecule is still prominent when compared to gas phase studies. This affects mostly the electronic but also the vibrational spectra. The matrix effects on the outcome of a spectrum can be divided in three categories: inhomogeneous broadening, shifting, and splitting of lines.[12–14]

As a different approach, the interaction can be weakened by supporting the guest molecule on a rare gas surface. This challenging technique can alternatively be realized by using large rare gas clusters instead of bulk matrices. Indeed, due to their solid state, the doping of such clusters after their formation via a pickup process limits the possible localization of the chromophore to surfaces sites.[15] Restricting the occupation of the host cluster to one guest molecule provides samples with isolated molecules. Multiple doping of rare gas clusters in order to increase target density carries the risk to form dimers or oligomers. Indeed, atoms and small molecules (<10 atoms) are mobile on the surface of rare gas clusters[16] so that in the case of heterogeneous doping of clusters, it could be shown that these clusters can serve as a chemical reaction center for the formation of complexes.[17] More recently, the formation of barium-xenon exciplexes on the surface of large argon clusters could be demonstrated.[18] However, recent measurements in our group pointed out that this surface mobility does not apply to larger PAHs such as PTCDA and that the molecules stay isolated from each other.[15]

The chromophore used in the present work is the PTCDA molecule ($C_{24}H_8O_6$). The ability of this perylene derivative to form highly ordered structures on surfaces[19,20] made it very popular in opto-organic applications and resulted in a large number of spectroscopic studies on a variety of substrates. Moreover, molecules of this type embedded in helium nanodroplets have already been extensively characterized in our group.[21–24]

The present paper is the second part of the spectroscopic study of PTCDA attached to rare gas samples and is devoted to fluorescence emission measurements (absorption and excitation measurements are presented in Ref. 15, later referred

to as Paper I). It is structured as follows: first, the fluorescence emission spectroscopy of single PTCDA molecules attached to large argon, neon or para-hydrogen clusters is presented. The complexes are excited at different vibronic levels in order to give an insight on the relaxation process of such complexes. The measurements are then compared to those obtained with PTCDA-doped superfluid helium droplets. Second, the fluorescence emission spectroscopy of PTCDA embedded in argon and neon matrices is presented and compared with absorption measurements. The comparison between rare gas clusters and rare gas matrices allows one to comment on the different effects of the crystal structure and of surface vs. inside localization of the chromophore on the spectral signatures. The presented measurements also bridge the gap between measurements obtained in the gas phase or with rare gas clusters and those obtained on surfaces or in the bulk.

II. EXPERIMENTAL SETUP

The experimental setup used for the production of clusters as well as their doping with PTCDA and their spectroscopic study has been thoroughly presented in Paper I and is here only briefly described. Large argon, neon, and para-hydrogen clusters as well as helium droplets are obtained via supersonic expansion of high-pressurized gas through a cold nozzle (a few tens of μm). Normal hydrogen is converted into para-hydrogen with the help of an *in situ* catalytic converter. However, in the course of the measurements presented here no differences in the spectral features have been found dependent on the different spin entities of the hydrogen molecule. With the expansion parameters used, the argon, neon, and para-hydrogen clusters have mean sizes of 450 atoms, 6 000 atoms, and 14 000 molecules, respectively; all of the formed clusters are solid in contrast to helium droplets which are superfluid (mean size of about 20 000 atoms per droplet).[25] The clusters are doped via a pickup process when traversing through a heated cell containing an adjustable partial pressure of PTCDA (Sigma Aldrich, used without further purification). The doping process is governed by Poissonian statistics (see Ref. [26] and references therein). The effect of multiple doping of large argon, neon, and hydrogen clusters with PTCDA is discussed in Paper 1. Within the instrument resolution no changes of spectral signatures can be assigned to PTCDA-PTCDA interactions or oligomer formation.

The doped clusters are excited by tunable laser radiation (pulsed dye laser Sirah Cobra, dye: Coumarin 102, repetition rate: 1 kHz, pulse duration: 10 ns, spectral resolution: <0.1 cm^{-1}) and the resulting fluorescence emission light is imaged onto an optical fiber bundle. The exit of this fiber bundle is mounted at the entrance slit of a spectrograph (Jobin-Yvon: SPEX 270M, grating: 1200 lines/mm). A telescope adapts the numerical aperture of the bundle with the one of the spectrograph. The emitted signal is recorded by a charge coupled device camera (CCD, Andor, Newton) fixed on the exit aperture of the spectrograph. The resolution of the setup was measured to be 18 cm^{-1} full-width at half maximum (FWHM).

Rare gas bulk matrices are produced by co-deposition of rare gas atoms and PTCDA molecules on a cold substrate (8 K for neon and 28 K for argon matrices; the other deposition parameters are discussed in Paper I). The matrices have a typical thickness of about 50 μm and a surface of a few square mm. Fluorescence measurements are obtained by focusing a laser beam (wavelength 473 nm) perpendicular to the matrix surface. The fluorescence light is collected by an optical fiber placed at the side of the matrix perpendicular to the laser beam. The output of the fiber is coupled to a spectrograph (Jobin-Yvon T64000, CCD Spectrum One). This arrangement ensures that only the fluorescence light is collected. The spectral resolution of the system using a 2400 lines/mm grating is 0.5 cm^{-1}.

III. EXPERIMENTAL RESULTS

A. Emission spectra of PTCDA-doped clusters

1. Emission of PTCDA embedded in helium nanodroplets

Figure 1 shows the fluorescence emission spectra of single PTCDA molecules embedded in helium droplets. The spectra are recorded at two different excitation energies, at 20 987.8 cm^{-1} (Fig. 1(b)) corresponding to the 0-0 line of the $S_1 \leftarrow S_0$ transition and at 21 217.3 cm^{-1} (Fig. 1(a)) corresponding to the first vibronic band. Spectra are compared to the laser-induced fluorescence (LIF) absorption spectrum mirrored with respect to the 0-0 line and artificially broadened with a Gaussian distribution taking into account the inferior resolution of the optical system (Fig. 1(c)). The fluorescence emission spectra are to a large extent identical to the mirrored absorption spectrum. The relative positions of the different vibronic lines only show weak deviations for modes at lower energies, which are due to discrepancies in the calibration procedure. The similarity between the fluorescence emission spectra and the mirrored absorption LIF spectrum means that electronic ground and excited potential energy curves are similar. This was already clear from the comparison between the LIF and Raman spectra of PTCDA.[22, 27] The relative intensities are also very similar in both fluorescence emission spectra and in the mirrored LIF spectrum except for the 0-0 transition which has slightly more intensity in the absorption spectrum. The line widths of the emission spectra are determined by the spectrometer, so only an upper limit can be deduced from the spectra. Previous studies on Phthalocyanine embedded in helium droplets showed a typical FWHM of about 1 cm^{-1}, comparable to the LIF absorption measurements.[28] One might expect a similar behavior for PTCDA molecules probed in the present experiment.

The excitation of the first vibronic mode (Fig. 1(a)) does not result in a fluorescence at this energy (dashed line in Fig. 1(a)) but leads to an unshifted spectrum when compared to the 0-0 excitation. This indicates a fast non-radiative relaxation process into the ground level of the excited state S_1 from which the fluorescence process into the ground state S_0 takes place. We measured the radiative lifetime for this transition to 5.5 ± 0.5 ns (see Ref. [29] for the method).

From the results on fluorescence emission spectroscopy of Mg-phthalocyanine, a similar process has been concluded. However, for that molecule the excitation of higher vibronic
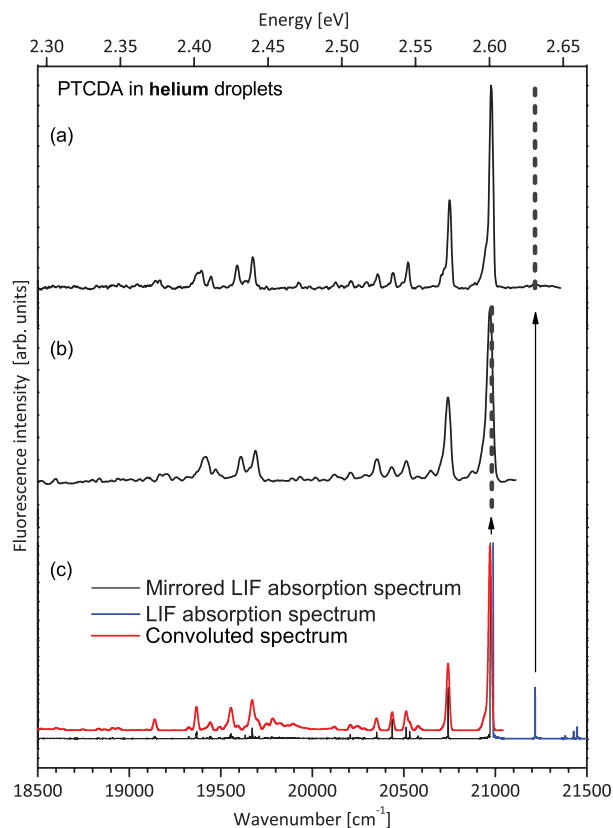
FIG. 1. Fluorescence emission spectra of PTCDA molecules embedded in helium droplets. Two excitation energies were probed: the 0-0 line of the $S_1 \leftarrow S_0$ transition at $20\,987.8$ cm^{-1} (b) and the first vibronic band at $21\,217.3$ cm^{-1} (a). These spectra are identical to the mirrored LIF spectrum (c), convoluted with a Gaussian distribution (FWHM = 18 cm^{-1}) taking into account the inferior resolution of the spectrograph-CCD system.
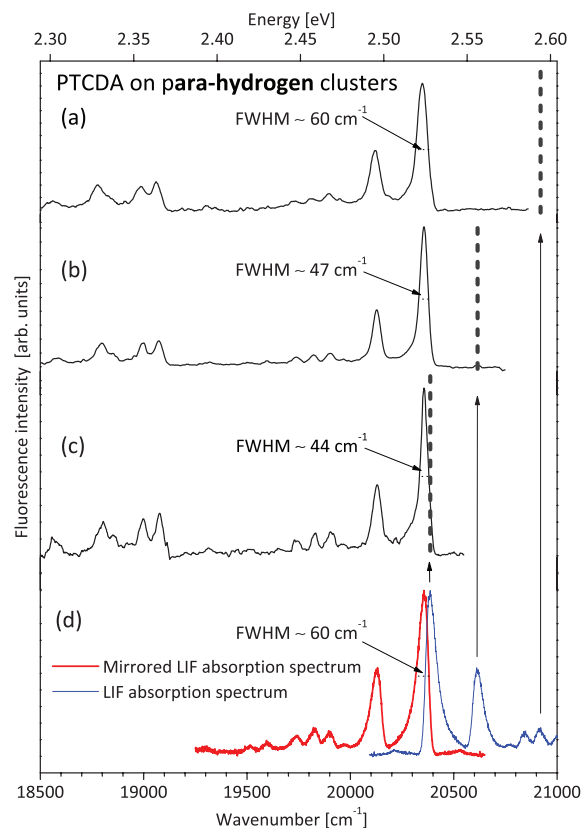
FIG. 2. Fluorescence emission spectra of PTCDA molecules attached to large para-hydrogen clusters. Three excitation energies (dashed lines) are probed: a radial stretching mode of C–C bonds at $20\,920$ cm^{-1} (a), the first vibronic band at $20\,615$ cm^{-1} (b) (breathing mode) and the 0-0 line at $20\,386$ cm^{-1} (c).

modes results in a splitting of the lines in the fluorescence spectrum. This was interpreted not to be originated from radiating higher vibronic levels, but related to different helium solvation configurations around the molecule.[28] Such a splitting, if present, would not be observable in our experiment because of the spectral resolution of the instrument.

2. Large para-hydrogen clusters

Similar to the measurements on helium droplets, fluorescence emission spectroscopy of PTCDA attached to large para-hydrogen clusters has been performed. In Fig. 2, the results are displayed for three different excitation energies. The emission spectrum obtained upon the excitation of the 0-0 line at $20\,386$ cm^{-1} (Fig. 2(c)) is identical to the mirrored LIF spectrum (Fig. 2(d)). Both the relative positions and relative intensities match. The only difference observed is the spectral resolution. A FWHM of about 44 cm^{-1}, identical for each peak is obtained, which is notably smaller than the value obtained in the LIF absorption spectrum (60 cm^{-1}), but still larger when compared to the resolution of the instrument. An extra broadening mechanism in the absorption spectrum is expected to originate from the strongly reduced lifetime due to the vibrational relaxation which increases at higher excitation energies due to the increasing number of relaxation channels.

The fluorescence emission spectrum for the excitation of the first vibronic band of the S_1 state is shown in Fig. 2(b). The excess energy of 230 cm^{-1} compared to the 0-0 transition is, as in the helium spectrum, completely dissipated prior to the radiative decay. The only difference observed is a slight increase of the FWHM to 47 cm^{-1}. For an even larger excess energy value (534 cm^{-1}), which corresponds to the vibronic mode at $20\,920$ cm^{-1} in the LIF spectrum (radial stretching mode of C–C bonds; Fig. 2(a)), the spectrum is again identical to the others, now having an increased FWHM of about 60 cm^{-1}. Taking into account the broadening coming from the spectrograph, still the effective line widths are smaller compared to the absorption measurements. An increase of the FWHM with the excess energy was also observed in the fluorescence emission spectra of perylene in an argon supersonic jet.[30] In that case, it was observed that an excess energy of 1600 cm^{-1} results in an increase of the FWHM of the peaks from $\sim$10 to $\sim$220 cm^{-1}. This broadening of the optical features with the excess excitation energy was interpreted by an increased number of relaxation paths to the ground state and/or due to extra non-radiative decay channels in the electronically excited state. Since in our case the vibrations of the PTCDA are relaxed prior to the emission, the increased line width may indicate a local heating of the environment due to the dissipated vibrational energy of the PTCDA. It might be interesting to note that the pulse width of the laser is roughly
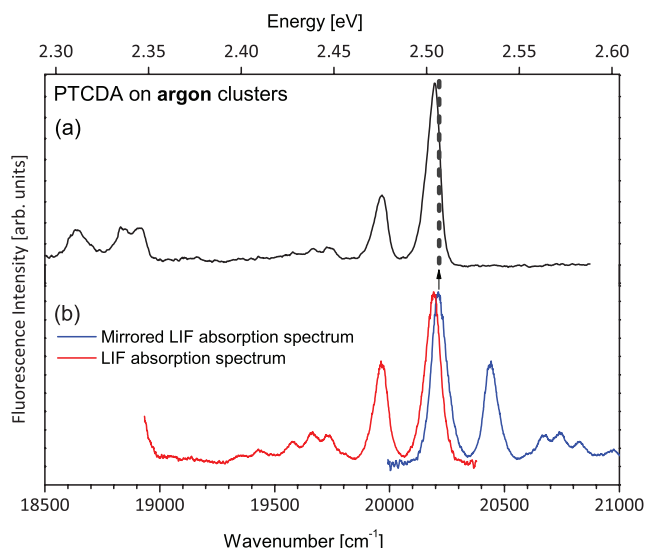
FIG. 3. Fluorescence emission spectra of PTCDA molecules attached to large argon clusters (a) compared with the mirrored LIF absorption spectrum (b). Excitation at the 0-0 line at 20 216 cm^{-1} is probed.
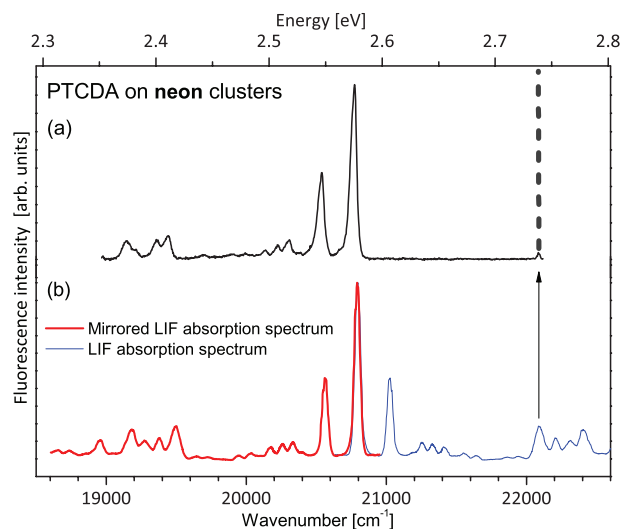

FIG. 4. Fluorescence emission spectra of PTCDA molecules attached to large neon clusters for the excitation energies corresponding to the vibronic mode at 22 088 cm^{-1} (a) in comparison with the mirrored LIF absorption spectrum (b). The small peak at 22 088 cm^{-1} in (a) can be assigned unambiguously to stray light from the laser beam.

the same as the radiation life time of PTCDA which does not allow heating processes by cycling transitions.

Similar to the measurements in helium droplets, no hot bands are observed upon the excitation of higher vibronic levels. Therefore, also the vibronic excited molecules attached to para-hydrogen clusters exhibit a fast non-radiative decay into the vibrational ground level of the S_1 state, followed by a radiative transition into the S_0 state. It has to be noted that we see no indication for any fluorescence quenching by the hydrogen environment, as has been observed in alkalis attached to hydrogen clusters.[31]

3. Large argon and neon clusters

The fluorescence emission spectrum of PTCDA attached to large argon clusters is displayed in Fig. 3(a) for the excitation of the 0-0 transition (20 216 cm^{-1}). This spectrum is similarly compared to the mirrored LIF absorption spectrum (Fig. 3(b)). For PTCDA attached to large neon clusters, four fluorescence emission spectra have been recorded, for four different excitation energies: the 0-0 transition at 20 797 cm^{-1}, the first vibronic band at 21 024 cm^{-1}, a radial stretching mode of C–C bonds at 21 330 cm^{-1}, and a deformation mode of C–H bonds at 22 088 cm^{-1}. The four recorded spectra are identical so only the one corresponding to the vibronic mode at 22 088 cm^{-1} is displayed in Fig. 4(a). For both argon and neon clusters, the relative positions, and relative intensities of the different peaks are independent of the excitation energy. In contrast to the measurements with para-hydrogen, only a slight increase of the FWHM of a few wavenumbers with the excess energy is observed. Note that for argon as for neon the line width remains below those of the corresponding absorption measurements. Furthermore, neon clusters exhibit significantly less broadening when compared to argon which is expected from the weaker interaction. Again, the excitation of higher vibronic levels does not result

in any hot band emission. The small peak at 22 088 cm^{-1} in Fig. 4(a) is unambiguously assigned to the Rayleigh scattering of the excitation laser on the cluster beam and is also observed with an identical intensity for an undoped neon cluster beam.

B. Fluorescence in a rare gas bulk matrix

1. Neon matrix

The fluorescence emission spectrum of PTCDA embedded in a neon matrix is displayed in the upper part of Fig. 5 and is much more complex when compared to the prior spectra of molecules attached to clusters. The absorption spectrum of the same sample is also shown (red line), mirrored with respect to the laser excitation line at 21 140 cm^{-1} and shifted to the red by 101 cm^{-1} for easier comparison. The first striking observation is the increase of the spectral resolution by more than one order of magnitude for the emission spectrum (FWHM of about 16 cm^{-1}) when compared to the absorption spectrum. The broadening of the latter is thought to be due to overlapping of individual vibrational bands in the excited states of different site isomers and extra line broadening as discussed above.

Apart from a different broadening, both the mirrored absorption spectrum and the fluorescence spectrum show the same profile. Each subfeature of the mirrored absorption spectrum can be related to different peaks of the fluorescence spectrum. The interaction of the molecule with the neon host leads to splitting, shifting, and broadening of lines. The PTCDA molecule apparently can bind to a well defined number of different sites in the neon host resulting in different shifts.[11] Unlike small embedded atoms or molecules, a large molecule substitutes a considerable number of host atoms leading to a significant number of host guest combinations. Such site isomers are characterized by different interaction strength with the matrix, resulting in a splitting of the spectral response
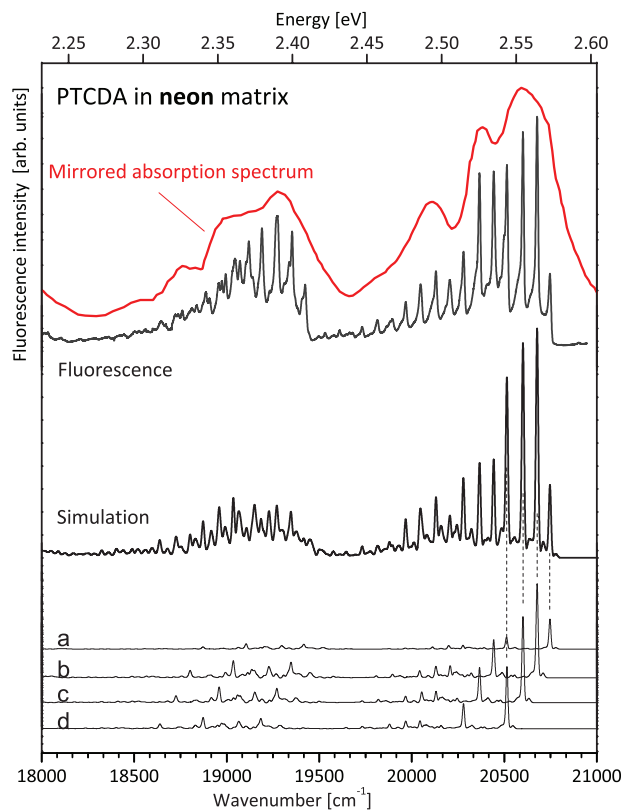
FIG. 5. Fluorescence emission spectrum of PTCDA molecules embedded in a neon matrix (top) compared with the mirrored absorption spectrum of the same matrix (red line). This spectrum can be reproduced (middle) by mixing four replicas of the excitation spectrum of PTCDA in the helium droplet with well-adjusted shifts and weighting factors (bottom).
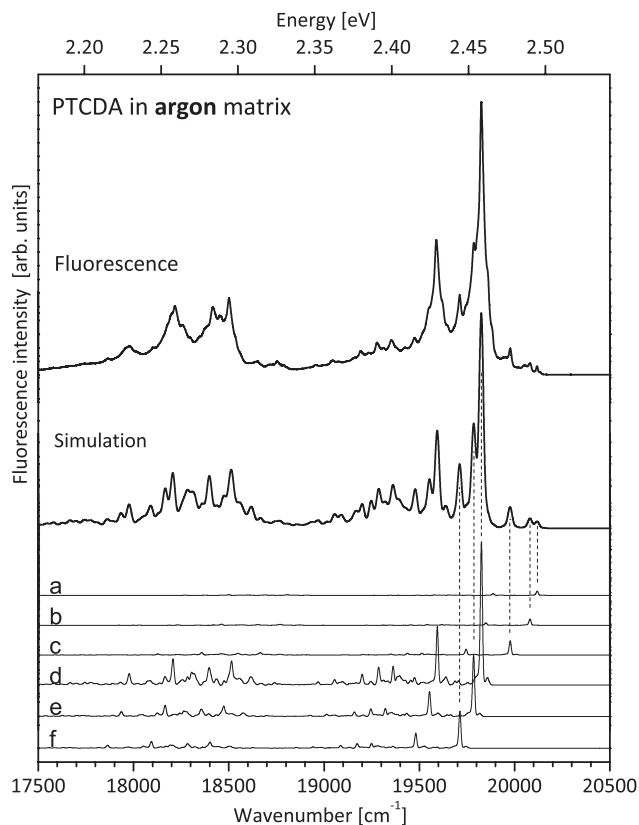

FIG. 6. Fluorescence emission spectra of PTCDA molecules embedded in an argon matrix (top). This spectrum can be reproduced (middle) by mixing six replicas of excitation spectrum of PTCDA in the helium droplet with corresponding shifts and weighting factors (bottom).

into multiple components having different relative intensities depending on their relative abundance. The absorption spectra of perylene, a similar molecule to PTCDA, has been measured in rare gas matrices too and showed a splitting of the main features. Each main transition was split into two components in a neon matrix, into five in an argon matrix, and six into a krypton matrix.[11,32] It is interesting to note that such well separated spectra of selected site isomers are not present when using rare gas clusters. Due to the surface localization of the chromophores the overall interaction is much weaker and no surrounding "cage" is present. The resulting differences of possible different binding sites are apparently much smaller when compared to the vibrational structure of the molecule and not resolved in the experiment.

Following the idea of splitting, the spectrum can be reproduced by superimposing identical replicas of a reference spectrum of PTCDA (Fig. 5, middle). The reference spectrum used is the LIF spectrum of PTCDA embedded in helium droplets (see Fig. 1(c)) which has been mirrored with respect to the 0-0 line of the $S_1 \leftarrow S_0$ transition. The mirrored spectrum has been convoluted with a Gaussian distribution to allow for matrix broadening. In solid neon, only four replicas, shifted and with different intensities, are sufficient to reproduce the experimental spectrum. In this way, the spectrum can be well simulated. The four replicas—a to d at the bottom of Fig. 5 —used to reproduce the neon matrix absorption spectrum are redshifted by 241, 310.5, 387, and 473.5 cm^{-1} with respect to

the 0-0 line of PTCDA in helium droplets at 20 987.8 cm^{-1}, respectively, and have weighting factors of 11%, 34%, 32%, and 23%, respectively. The typical error in the matrix spectrum is of ± 0.5 cm^{-1}. Note that the less intense peaks, in particular in the range between 20 300 and 20 000 cm^{-1} would ask for an increased number of replicas. Furthermore, some discrepancies in the relative intensity of some peaks (between 19 200 and 19 300 cm^{-1} and around 20 400 cm^{-1}) cannot be understood in our simplified simulation. Still, the overall agreement is satisfactory for an unambiguous assignment of each of the main features observed to different vibration modes of different site isomers of PTCDA molecules embedded in the neon matrix.

2. Argon matrix

The fluorescence emission spectrum in a solid argon matrix is shown in Fig. 6 and evidently demonstrates the stronger host-guest interaction by an enhanced redshift of roughly 800 cm^{-1} when compared to the neon matrix spectrum. The relative shift is similar to that found for perylene (788 cm^{-1}).[11] The broadening of the individual constituents is about 25 cm^{-1} which also is significantly enhanced when compared to neon (16 cm^{-1}). The larger perturbation of the spectra can be related to a stronger interaction between the chromophore and the matrix, mainly caused by a larger polarizability.[3,32]

Beside the interaction strength, the matrix temperature is known to play an important role on line widths. Crépin *et al.* showed for 9,10-dichloroanthracene in argon matrices that the typical line width varies between 12 cm^{-1} at 12 K and up to 30-40 cm^{-1} at 25 K.[8] Due to the widths of the different peaks and their proximity to each other, it is not possible to evaluate the line shapes and their possible asymmetry. In the present studies, we were not able to record an absorption spectrum due to the weak transmission of our argon matrix caused by smaller grain sizes compared to neon matrices resulting in stronger light scattering.[15,33]

Employing the same procedure as for neon, the argon spectrum can be reproduced with six replicas of the mirrored LIF spectrum of PTCDA in helium droplets convoluted with a Gaussian distribution 25 cm^{-1} in width. These (cf. a–f at the bottom of Fig. 6) have redshift values of 869, 907, 1011, 1162, 1203, and 1275 cm^{-1}, again compared to the origin of the $S_1 \leftarrow S_0$ transition of PTCDA in helium droplets at 20 987.8 cm^{-1}. Weighting factors are 1.6%, 2.4%, 5.4%, 53.6%, 23.1%, and 13.9%, respectively. It should be noted here that most of the intensity is due to only 3 replicas, giving more than 90% of the amplitude of the simulated spectrum. One might speculate that due to the higher temperature of the argon matrix (28 K, neon: 8 K), rearrangement effects are more favorable, resulting in a higher population of low energy conformations.[11]

IV. CONCLUSION

This paper presents fluorescence emission spectra of PTCDA attached to weakly interacting media. Single PTCDA molecules were attached to large argon, neon, and para-hydrogen clusters. The excitation of the 0-0 line of the $S_1 \leftarrow S_0$ transition results in similar fluorescence spectra for the different clusters used, only distinguished by different redshifts and line widths which are characterized in this study. Comparison with the mirrored excitation spectrum (LIF) shows an identical vibrational structure. The excitation of higher vibronic modes does not produce new spectral features, pointing to a fast relaxation of vibrational states compared to radiative processes. Furthermore, fluorescence emission spectra of PTCDA molecules embedded in argon and neon matrices have been recorded. The resolution of such spectra proved to be one order of magnitude better than corresponding absorption spectra. The many observed fluorescence lines have been successfully assigned to vibronic modes of different site isomers of PTCDA in the rare gas matrices. In conclusion, the combination of cluster and matrix spectra together with the well-resolved emission spectra of doped

matrices provide a conclusive assignment of the measured intensities. In particular also the relatively broader absorption spectra can be understood within the framework of the inhomogeneity of different site isomers.

[1] *Low Temperature Spectroscopy*, edited by B. Meyer (Elsevier, 1971).
[2] J. P. Toennies and A. F. Vilesov, Angew. Chem. Int. Ed. **43**, 2622 (2004).
[3] M. E. Jacox, J. Phys. Chem. Ref. Data **32**, 1 (2003).
[4] A. Sassara, G. Zerza, and M. Chergui, J. Phys. B **29**, 4997 (1996).
[5] F. Salama and L. J. Allamandola, J. Chem. Phys. **94**, 6964 (1991).
[6] F. Salama, C. Joblin, and L. J. Allamandola, J. Chem. Phys. **101**, 10252 (1994).
[7] T. M. Halasinski, D. M. Hudgins, F. Salama, L. J. Allamandola, and T. Bally, J. Phys. Chem. A **104**, 7484 (2000).
[8] C. Crépin and A. Tramer, Chem. Phys. Lett. **170**, 446 (1990).
[9] X. Chillier, P. Boulet, H. Chermette, F. Salama, and J. Weber, J. Chem. Phys. **115**, 1769 (2001).
[10] C. Joblin, F. Salama, and L. Allamandola, J. Chem. Phys. **102**, 9743 (1995).
[11] C. Joblin, F. Salama, and L. Allamandola, J. Chem. Phys. **110**, 7287 (1999).
[12] M. J. Almond and R. H. Orrin, Annu. Rep. Prog. Chem., Sect. C: Phys. Chem. **88**, 3 (1991).
[13] V. E. Bondybey, A. M. Smith, and J. Agreiter, Chem. Rev. **96**, 2113 (1996).
[14] *Physics and Chemistry at Low Temperatures*, edited by L. Khriachtchev (Pan Stanford, 2011).
[15] M. Dvorak, M. Müller, T. Knoblauch, O. Bünermann, A. Rydlo, S. Minniberger, W. Harbich, and F. Stienkemeier, J. Chem. Phys. **137**, 164301 (2012).
[16] A. Lallement, J. Cuvellier, J. M. Mestdagh, P. Meynadier, P. de Pujo, O. Sublemontier, J. P. Visticot, J. Berlande, and X. Biquard, Chem. Phys. Lett. **189**, 182 (1992).
[17] M. Briant, M. A. Gaveau, J. M. Mestdagh, and J. P. Visticot, J. Chem. Phys. **112**, 1744 (2000).
[18] M. Briant, M.-A. Gaveau, and J.-M. Mestdagh, J. Chem. Phys. **133**, 034306 (2010).
[19] F. Schreiber, Prog. Surf. Sci. **65**, 151 (2000).
[20] Q. H. Wang and M. C. Hersam, Nat. Chem. **1**, 206 (2009).
[21] M. Wewer and F. Stienkemeier, Phys. Rev. B **67**, 125201 (2003).
[22] M. Wewer and F. Stienkemeier, J. Chem. Phys. **120**, 1239 (2004).
[23] M. Wewer and F. Stienkemeier, Phys. Chem. Chem. Phys. **7**, 1171 (2005).
[24] J. Roden, A. Eisfeld, M. Dvorak, O. Bünermann, and F. Stienkemeier, J. Chem. Phys. **134**, 054907 (2011).
[25] S. Grebenev, J. P. Toennies, and A. F. Vilesov, Science **279**, 2083 (1998).
[26] O. Bünermann and F. Stienkemeier, Eur. Phys. J. D **61**, 645 (2011).
[27] R. Scholz, A. Kobitski, T. Kampen, M. Schreiber, D. Zahn, G. Jungnickel, M. Elstner, M. Sternberg, and T. Frauenheim, Phys. Rev. B **61**, 13659 (2000).
[28] R. Lehnig and A. Slenczka, J. Chem. Phys. **118**, 8256 (2003).
[29] O. Bünermann, Ph.D. dissertation, Universität Bielefeld, 2006.
[30] T. Imasaka, H. Fukuoka, T. Hayashi, and N. Ishibashi, Anal. Chim. Acta **156**, 111 (1984).
[31] C. Callegari, J. Higgins, F. Stienkemeier, and G. Scoles, J. Phys. Chem. A **102**, 95 (1998).
[32] I. Biktchantaev, V. Samartsev, and J. Sepiol, J. Lumin. **98**, 265 (2002).
[33] M. Klein and J. Venables, *Rare Gas Solids* (Academic, 1976).